Resonant tunneling through the repulsive Coulomb barrier of a quadruply charged molecular anion

Phuong Diem Dau,[1] Hong-Tao Liu,[1] Ji-Ping Yang,[2,3] Marc-Oliver Winghart,[2] Thomas J. A. Wolf,[2] Andreas-Neil Unterreiner,[2] Patrick Weis,[2] Yu-Run Miao,[4] Chuan-Gang Ning,[4,*] Manfred M. Kappes,[2,5,†] and Lai-Sheng Wang[1,‡]

[1]*Department of Chemistry, Brown University, Providence, Rhode Island 02912, USA*

[2]*Institut für Physikalische Chemie, Karlsruhe Institute of Technology, Kaiserstrasse 12, D-76128 Karlsruhe, Germany*

[3]*School of Electronic Science and Applied Physics, Hefei University of Technology, Hefei 230009, China*

[4]*Department of Physics, State Key Laboratory of Low-Dimensional Quantum Physics, Tsinghua University, Beijing 100084, China*

[5]*Institut für Nanotechnologie, Karlsruhe Institute of Technology, Postfach 3640, D-76021 Karlsruhe, Germany*

(Received 14 February 2012; published 25 June 2012)

Multiply charged anions possess a repulsive Coulomb barrier (RCB) against electron emission, thus allowing for long-lived metastable species with negative electron binding energies. For the prototypical multianion, bisdisulizole tetra-anion, we demonstrate that electronically excited states supported by the RCB can undergo resonant tunneling. The dynamics of this process was investigated by one-photon photoelectron imaging and femtosecond pump-probe photoelectron spectroscopy and confirmed by theoretical calculations. Efficient resonant tunneling emission of electrons from the excited states of multianions may be common for systems with sufficiently large RCB. This may provide new opportunities to study electron emission dynamics in complex systems.

DOI: 10.1103/PhysRevA.85.064503 PACS number(s): 33.60.+q, 33.80.Eh, 36.90.+f

Multiply charged anions (MCAs) are common in the condensed phase [1]. However, if the counterions or solvents are removed, isolated MCAs in the gas phase become rather fragile and exhibit many unique physical properties due to the strong intramolecular Coulomb repulsion [2–8]. When an electron is emitted from a MCA, it experiences a short-range attraction and a long-range repulsion from the remaining negative ion, resulting in a repulsive Coulomb barrier (RCB). The RCB provides dynamic stability to MCAs and allows long-lived metastable MCAs with negative electron binding energies to be observed [9–12]. Metastable MCAs can undergo spontaneous electron emission from their ground states by tunneling through the RCB, analogous to α decay for radioactive nuclei [11–16]. Such decay has been studied using ion trap mass spectrometry, yielding tunneling lifetimes on the order of seconds for a number of metastable MCAs at room temperature [11,12,16].

Photoelectron spectroscopy (PES) has been an important technique to probe the RCB and electronic stability of MCAs [7,9,17]. In PES of MCAs, the detachment photon energies must be higher than the RCB. In other words, no slow electrons can be observed in PES of MCAs: The outgoing electrons must have enough kinetic energy to overcome the RCB because the nonresonant tunneling probability is usually negligible except near the very top of the RCB. Thus, PES spectra of MCAs often display a cutoff at the high binding energy side. Such spectral cutoff is a unique feature of MCAs, allowing the RCB heights to be estimated [18]. However, if sufficiently long-lived excited states exist below the RCB, resonant tunneling can occur, producing electron detachment features beyond the spectral cutoff. Resonant tunneling was first suggested in PES of copper phthalocyanine tetrasulfonate tetra-anion [19], which was the first MCA observed to be metastable [9]. The related dynamics has been investigated by pump-probe photoelectron spectroscopy, as well as in a number of other phthalocyanine-based MCAs [20]. The latter study demonstrated that for certain metastable, phthalocyanine-based multianions, excited state electron tunneling detachment may become fast enough to compete with internal conversion. Such (resonant) tunneling from electronically excited states via the RCB of MCAs is interesting because it provides a unique opportunity to study electron emission and relaxation dynamics in complex systems. However, among the many MCAs studied so far, resonant tunneling is rare—it has only been inferred in the phthalocyanine family of molecules. In retrospect, two conditions must be met to allow resonant tunneling states. First, the RCB must be high enough to support an excited state. This usually means MCAs with more than two excess charges, which produce stronger intramolecular Coulomb repulsion and a higher RCB. Second, the parent molecule must have a rich manifold of excited states in the visible or near-ultraviolet spectral region.

Here we report a direct observation of a resonant tunneling state in the bisdisulizole tetra-anion [$BDSZ^{4-}$, see Fig. 1(a)], which was found to be a metastable MCA with a negative electron binding energy of -0.8 eV and a RCB of 4.3 eV. First, the $BDSZ^{4-}$ anion was studied using a magnetic-bottle PES apparatus and PE imaging. The tunneling state was observed to be at 3.2 eV above the ground state of the tetra-anion within the RCB. It was confirmed by theoretical calculations using the Wentzel-Kramers-Brillouin (WKB) theory and investigated by femtosecond pump-probe PES. This yielded a lifetime of 450 fs for the resonant tunneling state.

The PES experiment was performed with an electrospray PES apparatus equipped with a magnetic-bottle electron analyzer [17] and a velocity-map imaging detector [21]. The temporal dynamics of resonant states was investigated using femtosecond pump-probe PES [20]. The $BDSZ^{4-}$ anions were generated by electrospray of a 2 mM solution of Na-BDSZ dissolved in a mixed water and methanol solvent. Both the magnetic-bottle and imaging PES experiments were calibrated by the known spectra of Br^- and I^-. The electron kinetic energy resolution ($\Delta E/E$) was about 3%, i.e., ~30 meV for

*ningcg@mail.tsinghua.edu.cn
†Manfred.Kappes@kit.edu
‡Lai-Sheng_Wang@brown.edu

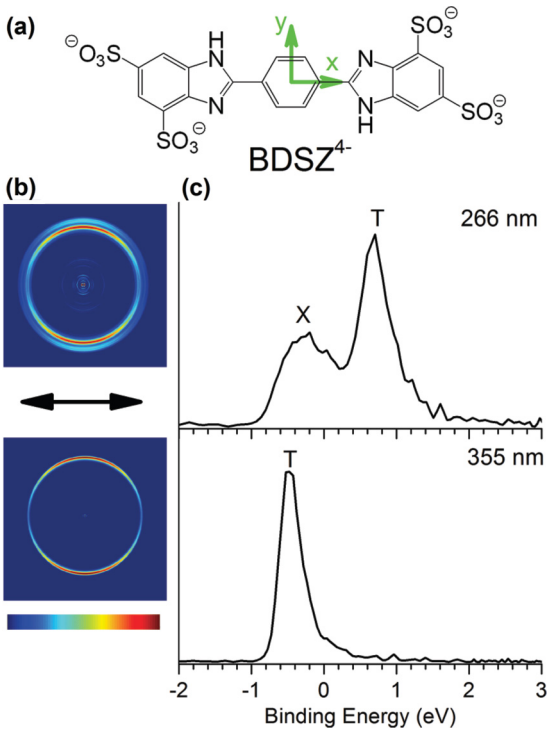

FIG. 1. (Color online) (a) Molecular structure of $BDSZ^{4-}$. (b) Photoelectron images of $BDSZ^{4-}$ at 266 nm (top) and 355 nm (bottom), showing the perpendicular intensity distributions relative to the laser polarization indicated by the arrows. (c) Photoelectron spectra of $BDSZ^{4-}$ converted from (b) by integrating the photoelectron intensity around the circular images after reverse-Abel transformation.

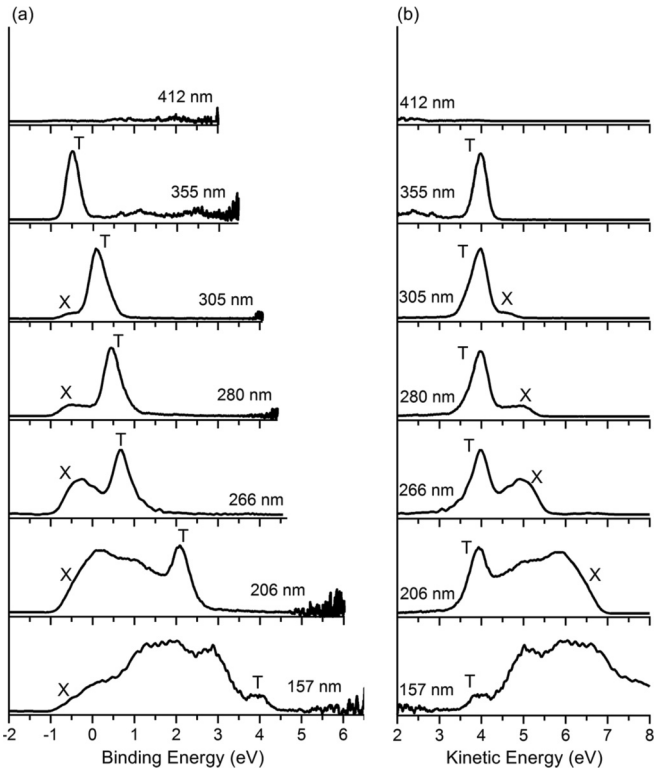

FIG. 2. Photoelectron spectra of bisdisulizole tetra-anion ($BDSZ^{4-}$) at 412 nm (3.01 eV), 355 nm (3.49 eV), 305 nm (4.09 eV), 280 nm (4.43 eV), 266 nm (4.66 eV), 206 nm (6.02 eV), and 157 nm (7.87 eV) plotted versus (a) the electron binding energy and (b) the photoelectron kinetic energy.

1.0-eV electrons. The corresponding energy resolution of the pump-probe apparatus was about 5%.

Figures 1(b) and 1(c) show the results of PE imaging of $BDSZ^{4-}$. These data were presented in a recent study as an example of perpendicular electron emission guided by the extra charges [22]. But the spectral features were not analyzed. The binding energy spectra [Fig. 1(c)] revealed that $BDSZ^{4-}$ is metastable with negative electron binding energies. Two spectral bands were observed at 266 nm [Fig. 1(c)]: a broad low-binding-energy band (X) with an adiabatic detachment energy (ADE) of -0.8 eV and a sharper feature (T) with a well-defined vertical detachment energy (VDE) of 0.7 eV. The 355-nm spectrum showed only one band: It was expected that the higher-binding-energy band at 266 nm would be cut off due to the RCB. However, the 355-nm spectrum was puzzling in two aspects: (1) The ADE of the band at 355 nm (–0.7 eV) was not consistent with that of band X in the 266-nm spectrum (–0.8 eV); (2) the band in the 355-nm spectrum did not resemble band X in the 266-nm spectrum, but rather appeared more like the higher-binding-energy band (T) shifted to a lower binding energy. To better understand these spectral features and their photon energy dependence, we studied $BDSZ^{4-}$ with our magnetic-bottle PES apparatus at a more extended photon energy range using a Nd:YAG laser (355 and 266 nm), a tunable dye laser (412, 305, 280, and 206 nm), and an F2 excimer laser (157 nm).

The more extended PES data set is displayed in Fig. 2(a). At 157 nm (7.87 eV), broad and near-continuous spectral features were observed between -1 and 4 eV. At 206 nm (6.02 eV), spectral features above 2.5 eV were cut off due to the RCB, as expected. However, a relatively sharp band (T) appeared at the high-binding-energy side. As the photon energy continued to decrease, more spectral features were cut off, but a sharp band on the high-binding-energy side seemed to be present in all the spectra down to 355 nm. Finally, at 412 nm (3.01 eV), no photoelectron signals were observed, suggesting the photon energy must be below the RCB. Surprisingly, when we plotted the PES spectra in kinetic energies [Fig. 2(b)], we found that the high-binding-energy feature (T) lined up in all the spectra with the same nominal kinetic energy of 4.0 eV, including the weak high-binding-energy feature in the 157-nm spectrum.

This feature (T) could not come from direct photodetachment. The same kinetic energy at different detachment photon energies suggested that this band came from the same autodetachment state, i.e., a resonant tunneling state within the RCB. How was this resonant state produced in the first place? BDSZ is a well-known, strong UV absorber used commercially in sunscreens [23]. In aqueous solution, it has a strong UV absorption band centered at 335 nm (with an onset near 380 nm), overlapping with other higher-energy-absorption features [23]. Thus, no matter what UV wavelengths were used in the photodetachment, a resonant absorption occurred to produce a highly excited tetra-anion, $(BSDZ^{4-})^*$, which then relaxed to a common lower state (most likely the lowest singlet excited state), from which resonant tunneling took place. The PES spectral features with kinetic energies higher than the

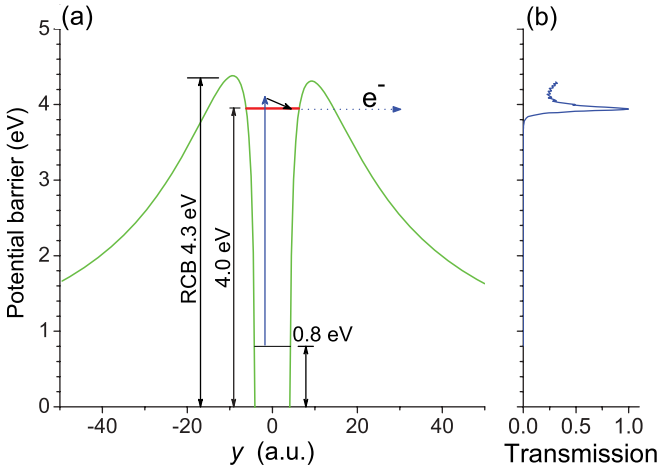

FIG. 3. (Color online) (a) The model repulsive Coulomb potential used for calculating the energy level and lifetime of the resonant state with WKB theory. The distance is in atomic units (1 a.u. = 0.529 Å). The marked energy levels were determined from the observed photoelectron spectra. The vertical blue arrow stands for the excitation from a valence state to an excited state of $BDSZ^{4-}$, and the resonant tunneling state is represented by the red horizontal line. The dotted arrow indicates the electron tunneling. (b) Transmission yield calculated using WKB theory for the model barrier potential and resonant tunneling state indicated vs the emitted electron energy. The peak at 4.0 eV reflects the resonant state within the RCB.

tunneling signals come from direct photodetachment, which cannot compete with resonant tunneling as the photon energy is decreased.

From the true spectral cutoff, we estimated a RCB height of 4.3 eV based on the 157-nm spectrum, where the resonant tunneling signal was relatively weak. The ADE for $BDSZ^{4-}$ can only be evaluated from the spectra at photon energies above 355 nm, because the 355-nm spectrum was entirely due to the resonant tunneling state. The ADE of $BDSZ^{4-}$ was estimated as -0.8 eV from the 266-nm spectrum. Based on the ADE of $BDSZ^{4-}$ and the 4.0-eV nominal kinetic energy of the resonant tunneling band, we estimated that the tunneling state is about ~3.2 eV above the ground state of the tetra-anion and ~0.3 eV below the RCB top, as shown schematically in Fig. 3(a). The 412-nm (3.01-eV) detachment energy was below the RCB and was also below the resonant state. Thus, no electron signals were observed at this detachment wavelength (Fig. 2).

It should be noted that the angular distribution of the electrons corresponding to the resonant tunneling band is highly perpendicular. As shown in Fig. 1(b), the photoelectron intensity at the direction perpendicular to the laser polarization is much stronger than in the direction parallel to the laser polarization. The perpendicular angular distribution is due to the anisotropy of the RCB caused by the terminal negative charges, because the electrons are emitted from molecular orbitals in the middle of the $BDSZ^{4-}$ anion [Fig. 1(a)], as reported recently [22]. The observed highly anisotropic electron distribution also means that the resonant tunneling is a very fast process, relative to the rotational period of $BDSZ^{4-}$. The rotational constant B of $BDSZ^{4-}$ for the rotation around its C_2 symmetry axis was calculated to be 0.017 GHz [24]. At room temperature ($T = 300$ K), the population at various rotational levels is governed by the Boltzmann distribution, $\propto (2J+1)\exp[-hBJ(J+1)/kT]$, where k is the Boltzmann constant and h is the Planck constant. Thus, the most probable rotational quantum number $J_{\max} \approx (kT/2hB)^{1/2}$ or ~430, which has a rotational period of $t_r \approx 1/(2BJ_{\max}) \approx 6.8 \times 10^{-11}$ s (68 ps). Hence, the lifetime of the resonant tunneling state should be much shorter than 68 ps.

To quantitatively understand the resonant tunneling state in the RCB, we calculated the potential barrier for the emission of an electron from the highest occupied molecular orbital of $BDSZ^{4-}$, using the DFT-B3LYP/6-311++G** method [22,24] with the frozen static orbital approximation [25]. The lowest RCB is along the y axis, which is perpendicular to the long molecular axis [Fig. 1(a)], as expected. The calculated lowest RCB is 4.4 eV, in excellent agreement with the value estimated from the cutoff of the PES spectra (~4.3 eV). To simplify the calculation of electron tunneling with the WKB theory [26], a one-dimensional double barrier along the y axis was modeled to approximate the anisotropic RCB. An averaged potential inside the model barrier was taken as an adjustable parameter for producing the best agreement with the observed energy level of the resonant state. Indeed, we reproduced a resonant tunneling state with an energy level of 4.0 eV. Figure 3(b) shows the transmission curve versus the electron energy. Since the measured energy distribution of the tunneling state (T in Fig. 2) is a complicated convolution of Frank-Condon overlaps and vibrational excitations, as well as instrumental energy resolution, it cannot be used for estimating the lifetime. However, the simulated energy width of the resonant state ($\Delta E = 0.07$ eV) in Fig. 3(b) can be used to obtain a first-order estimate of the lifetime τ ($\tau \sim \hbar/\Delta E$) of the resonant state to be $\sim 10^{-14}$ s (~10 fs). The overall profile is not in good agreement with the measured energy distribution, which might be due to the oversimplified barrier model (in addition to the factors already mentioned above).

The temporal dynamics of the resonant state in $BDSZ^{4-}$ was directly investigated using femtosecond PES [20]. The pump and probe laser pulses were provided using a fully integrated 1 kHz Ti:sapphire femtosecond laser system (Clark-MXR, CPA-2001), which can yield 775-nm (1.6-eV) pulses with an overall pulse energy of 1 mJ. After second harmonic generation, pump (388-nm, 3.2-eV) and probe (775-nm) laser pulses were separated and delayed relative to each other using a computer-controlled optical delay line (Nanomover, Melles Griot). For time-resolved PES, typical pump pulse energies were 20 μJ in order to minimize two-photon detachment. Probe pulse energies were typically 120–140 μJ. The pump-probe time resolution in the detachment region of the PE spectrometer was determined as 440 ± 30 fs by cross-correlation measurements of pump and probe laser beams [see the dashed curve in Fig. 4(b)].

Figure 4(a) shows the pump-probe results for $BDSZ^{4-}$. The strong peak in the photoelectron intensity at an electron kinetic energy of 4.0 eV corresponds to the resonant tunneling signal resulting from the $BDSZ^{4-}$ molecules, which have absorbed one photon from the 388-nm pump radiation. The weaker signal in the kinetic energy range from 4.6 to 5.7 eV corresponds to the two-color pump-probe transient

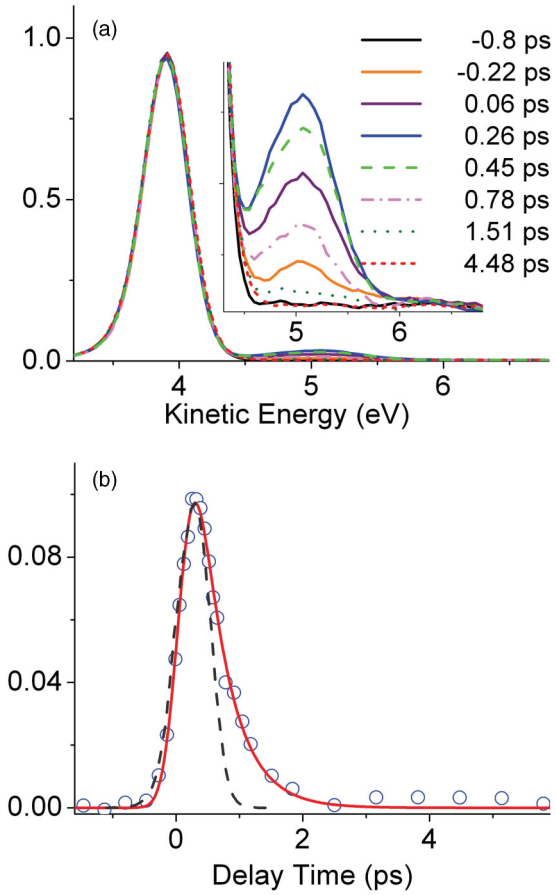

FIG. 4. (Color online) (a) Pump-probe photoelectron spectra of $BDSZ^{4-}$ at the indicated delay times. The inset displays an expanded scale (15 ×) of the transient signal corresponding to photodetachment from the tunneling state. (b) (Blue circles) integrated photoelectron signals from the 4.6–5.7 eV transient region vs the pump-probe delay; (red line) a single exponential fit; (black dashed line) time resolution from laser cross-correlation measurement (both in arbitrary units).

process. Here interaction with a 775-nm probe photon leads to photodetachment of electrons from the 3.2-eV transient resonant tunneling state—as prepared by the absorption of one pump photon. The inset in Fig. 4(a) displays more details of the pump-probe transient signal and the associated dynamics. With increasing pump-probe delay, the transient signal rapidly decays as population is lost from the 3.2-eV tunneling state. No transient signal is observed for pump-probe delays beyond 4.48 ps. Figure 4(b) shows the integrated transient signal intensity versus the pump-probe delay. This intensity curve was fitted with a single exponential decay to obtain the effective lifetime of the tunneling state by also taking into account the experimental time resolution. This yields a time constant of 450 ± 90 fs, which is comparable to the time resolution of the experiment. We note that this lifetime is consistent with the inference from the angular distributions, which show that tunneling emission from the 3.2-eV excited state is complete within a molecular rotational period. It is also consistent with (but somewhat above) the lifetime estimated from WKB theory using the model RCB.

In conclusion, resonant tunneling through the repulsive Coulomb barrier of a quadruply charged anion has been explored. The energetics and dynamics of the resonant state were investigated using one-photon photoelectron spectroscopy and imaging, theoretical calculations, and two-color, time-resolved pump-probe photoelectron spectroscopy. Resonant states within the RCB may be quite common in complex MCAs. Investigation of the resonant tunneling via RCB may open up new opportunities for investigating the unique properties of multiply charged anions and electron emission dynamics in complex systems.

ACKNOWLEDGMENTS

The experiments done at Brown were supported by the National Science Foundation (Grant No. CHE-1049717 to L.S.W.). The experiments done at KIT were supported by the Deutsche Forschungsgemeinschaft (CFN C3.2 to M.M.K.). M.Y.R. and N.C.G. would like to acknowledge the National Natural Science Foundation of China for partial support of this work (Grant No. 11174175).

[1] J. Simons, J. Phys. Chem. A **112**, 6401 (2008).
[2] S. N. Schauer, P. Williams, and R. N. Compton, Phys. Rev. Lett. **65**, 625 (1990).
[3] J. Kalcher and A. F. Sax, Chem. Rev. **94**, 2291 (1994).
[4] M. K. Scheller, R. N. Compton, and L. S. Cederbaum, Science **270**, 1160 (1995).
[5] A. I. Boldyrev, M. Gutowski, and J. Simons, Acc. Chem. Res. **29**, 497 (1996).
[6] G. R. Freeman and N. H. March, J. Phys. Chem. **100**, 4331 (1996).
[7] L. S. Wang and X. B. Wang, J. Phys. Chem. A **104**, 1978 (2000).
[8] A. Dreuw and L. S. Cederbaum, Chem. Rev. **102**, 181 (2002).
[9] X. B. Wang and L. S. Wang, Nature **400**, 245 (1999).
[10] S. Tomita *et al.*, J. Chem. Phys. **124**, 024310 (2006).
[11] K. Arnold, T. S. Balaban, M. N. Blom, O. T. Ehrler, S. Gilb, O. Hampe, J. E. v. Lier, J. M. Weber, and M. M. Kappes, J. Phys. Chem. A **107**, 794 (2003).
[12] X. B. Wang, A. P. Sergeeva, X. P. Xing, M. Massaout, T. Karpuschkin, O. Hampe, A. I. Boldyrev, M. M. Kappes, and L. S. Wang, J. Am. Chem. Soc. **131**, 9836 (2009).
[13] R. N. Compton, A. A. Tuinman, C. E. Klots, M. R. Pederson, and D. C. Patton, Phys. Rev. Lett. **78**, 4367 (1997).
[14] X. B. Wang, C. F. Ding, and L. S. Wang, Chem. Phys. Lett. **307**, 391 (1999).
[15] M. N. Blom, O. Hampe, S. Gilb, P. Weis, and M. M. Kappe, J. Chem. Phys. **115**, 3690 (2001).
[16] S. Panja *et al.*, J. Chem. Phys. **127**, 124301 (2007).
[17] L. S. Wang, C. F. Ding, X. B. Wang, and S. E. Barlow, Rev. Sci. Instrum. **70**, 1957 (1999).
[18] L. S. Wang, C. F. Ding, X. B. Wang, and J. B. Nicholas, Phys. Rev. Lett. **81**, 2667 (1998).
[19] X. B. Wang, K. Ferris, and L. S. Wang, J. Phys. Chem. A **104**, 25 (2000).
[20] O. T. Ehrler, J. P. Yang, A. B. Sugiharto, A. N. Unterreiner, and M. M. Kappes, J. Chem. Phys. **127**, 184301 (2007).

[21] X. P. Xing, X. B. Wang, and L. S. Wang, J. Chem. Phys. **130**, 074301 (2009).

[22] C. G. Ning, P. D. Dau, and L. S. Wang, Phys. Rev. Lett. **105**, 263001 (2010).

[23] http://products.symrise.com/fileadmin/user_upload/lifeessentials/pdf/NeoHeliopan-AP.pdf.

[24] The molecular structure was optimized with density functional theory (DFT) using the B3LYP functional with a 6-311 + + G** Pople basis set. The electron density distribution of each molecular orbital was also obtained with the B3LYP/6-311 + + G** method. The GAUSSIAN 03code was used for the calculation: M. J. Frisch *et al*., GAUSSIAN 03, revision E.01, Gaussian, Inc., Pittsburgh, PA, 2003.

[25] A. Dreuw and L. S. Cederbaum, Phys. Rev. A **63**, 049904(E) (2001).

[26] P. E. Hodgson, E. Gadioli, and E. G. Erba, *Introductory Nuclear Physics* (Oxford University Press, Oxford, 1997).